16th World Conference on Earthquake, 16WCEE 2017

Santiago Chile, January 9th to 13th 2017

Paper N° XXXX (Abstract ID)

Registration Code: S-XXXXXXXX

SEISMIC BEHAVIOR OF LOW-RISE URM STRUCTURES WITH GEOMETRIC VARIATION

J. Park [1]

[1] *Professor, Wonkwang University, Iksan, Jeonbuk 570-749, South Korea, Joonam.park@gmail.com*

Abstract

Seismic risk assessment of unreinforced masonry (URM) buildings is an important process for seismic retrofit of essential facilities located in the south and central US (CSUS) region, as more than 30% of the facilities are low-rise URM buildings. Although HAZUS provides a set of fragility curves for such structures as an essential tool for conducting the seismic risk assessment, the variation of the seismic performance level due to the geometric characteristics is not explicitly considered. This study investigates the effect of geometric variation of low-rise URM structures on the seismic fragility assessment. Utilizing the URM building inventory information within the CSUS region variables that describe the physical shape of an URM structure are identified. A simplified composite spring model developed for URM structures is then utilized to monitor the nonlinear seismic behavior. At last the seismic fragility curves corresponding to various configurations of the shape of URM structures are developed and compared. The analysis confirms that the length of the out-of-plane walls and the number of stories of URM buildings have significant effects on the seismic risk, whereas the perforation ratio does not affect much the seismic performance. It is suggested that using a single set of fragility curves is not adequate for seismic risk assessment of low-rise URM buildings unless the geometric variation is explicitly considered.

Keywords: unreinforced masonry, geometric variation, composite spring model

1. Introduction

Unreinforced masonry (URM) structures comprise a large portion of residential and/or essential structures in many areas. In particular, more than 30% of the essential facilities such as firehouses and police stations distributed over the central and southern United States (CSUS) region are URM structures [1,2]. In case of seismic events, URM structures sometimes cause significant losses due to its lack of seismic resistance and ductility. Moreover, seismic failure of essential facilities may cause secondary social and economic losses because additional rescue actions could not be provided.

Potential losses due to seismic failure or damage of existing structural systems could be mitigated through seismic retrofit of the structures. Seismic risk analysis must be preceded in order to make the most effectiveness in identification of seismically vulnerable structures and determination of the retrofit scheme. HAZUS, the seismic loss estimation package developed by the Federal Emergency Management Agency (FEMA), provides seismic fragility curves for various types of structures [3]. These fragility curves are for assessment of expected social and economic losses that may be caused by a scenario earthquake for a specific region. Seismic fragility curves for unreinforced masonry structures are also available in HAZUS for two categories – low-rise and mid-rise. That is, a single set of fragility curves is presented for representation of the seismic performance of the structures within a same category. Even in a same category, however, a wide variation exists in the size and the shape of the structures. The seismic performance would not be uniform among the structures but have some variations, too. Therefore, application of a single representative set of fragility curves for seismic retrofit of a single structure or some portion of the structures may not be adequate [4,5].

A number of studies on fragility analysis of URM structures can be found in the literature review. Bothara et al. [6] performed an experimental investigation on the seismic performance of a half-scaled two story URM structure. The fragility curves were developed based on the experimental result. Park et al. [4] analytically developed fragility curves representative of the low-rise URM buildings located in the central and southern United States. The result was then compared with the HAZUS fragility curves and a potential problem in using a representative fragility curves for an arbitrarily grouped structures was addressed. Agnihotri et al. [7] investigated the seismic performance of the out-of-plane walls of URM buildings with prior in-plane wall damage. A fragility analysis was also conducted considering the effect of the in-plane wall damage. Although many efforts were made for fragility analysis of URM buildings, none of them explicitly considered the effect of the geometric variation on the seismic fragility. This study investigates the effect of physical variation of low-rise URM structures on the seismic fragility assessment. Utilizing the URM building inventory information within the CSUS region [1] variables that describe the physical shape of an URM structure are identified. A simplified composite spring model developed for URM structures is then utilized to monitor the nonlinear seismic behavior. At last the fragility curves corresponding to various configurations of the shape of URM structures are compared and the tendency is discussed.

2. Geometric Variation of URM Structures

As mentioned above, currently available fragility curves for URM structures are developed without consideration of the variation of the seismic performance of the structures within a same classification. This study is motivated by the assumption that the seismic performance of URM structures varies depending on the variation of the geometric shape and dimensions although they fall into a same category. According to the HAZUS classification, single-story and two-story URM buildings are classified as low-rise whereas mid-rise URM means three-story URM buildings. Most URM buildings are low-rise. In particular, the inventory analysis for URM essential facilities located in the CSUS region indicates that more than 90% of the buildings are low-rise. Fig. 1 shows the distribution of the physical dimensions of the buildings. When the length of the longer side of a URM building is denoted L and the shorter side is denoted W, the distributions of L and W are shown in Fig. 1(b) and (c). The aspect ratio, which is L/W, is shown in Fig. 1(d). The variation in length of the URM buildings is expected to affect the seismic performance level considering that the lack of strength and excessive displacement of the out-of-plane walls (OWP) and the diaphragms are the direct cause of the seismic failure [2]. Moreover, the direction of the earthquake could play an important role because most of the lateral resistance against seismic loadings comes from the in-plane walls (IPW) [2, 8, 9].

Another variable that may affect the seismic performance level of URM structures is the perforation ratio of the IPW. The lateral stiffness and/or strength of the IPW would decrease as the area of the perforated region increases. Masonry piers that form due to the existence of the perforations are considered to be vulnerable to seismic loadings because of their weak lateral strength (Fig. 2). In fact the failure of masonry piers is one of the common seismic failure modes of URM buildings [10,11].

As mentioned above HAZUS classification defines the low-rise URM as single-story or two-story URM buildings. Theoretically, the first story of a two-story URM building is expected to undergo less seismic damage compared to a single-story building because the vertical load transferred from the second story increases the lateral strength of the first story. The seismic damage of the second story, however, will be greater than the single-story URM because of the response of the second story is amplified from the ground motion. Moreover, a two-story building will be affected by flexural behavior in addition to the lateral shear whereas a single-story building is mainly governed by the shear behavior only. Fragility analysis for URM buildings with various configurations of the geometric shape and size is presented in the following section to verify the assumptions mentioned above.

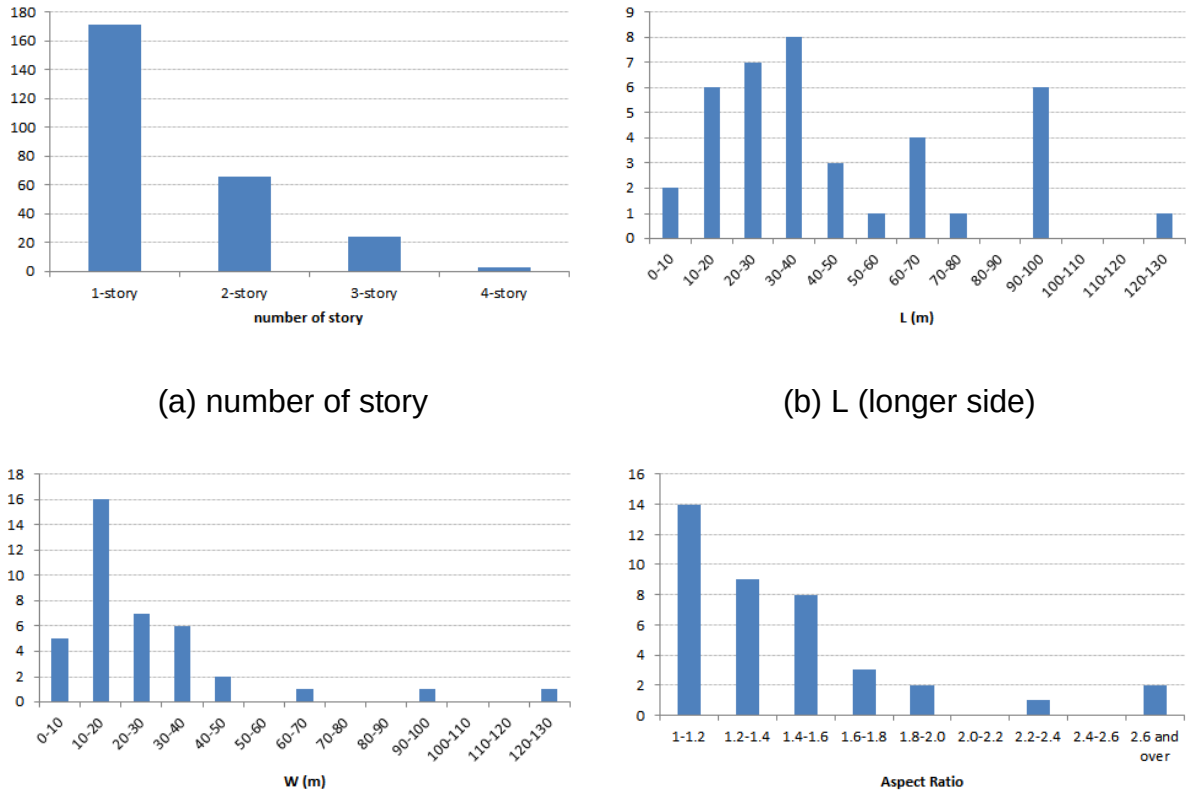

(a) number of story

(b) L (longer side)

(c) W (shorter side)

(d) aspect ratio

Fig. 1 – Frequency plots for URM buildings in Mid-America region

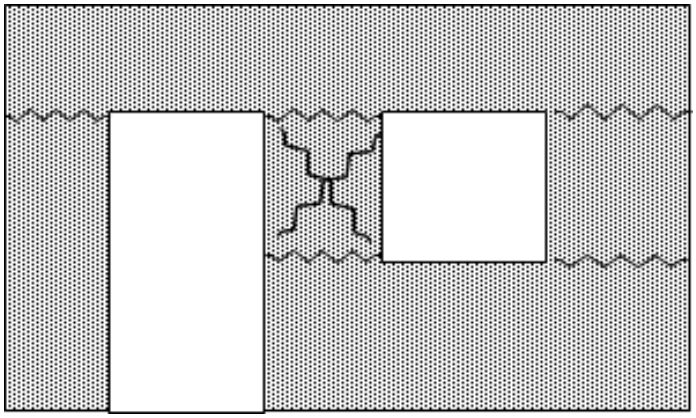

Fig. 2 – Example of seismic failure of masonry piers

3. Modeling of URM building

Masonry is composed of bricks and mortar. Compared to other materials such as steel or reinforced concrete, unreinforced masonry shows highly nonlinear behavior to lateral excitation such as earthquake loadings. The seismic response of URM becomes highly nonlinear once cracking develops along mortar joints and/or through bricks. Modeling the brick units with solid elements and the mortar joints with nonlinear interface elements would be the most refined approach for the analysis of URM structures under earthquake excitation [9]. This approach, however, is considered impractical in seismic risk analysis where a computer simulation with a large number of nonlinear analyses is necessary. Especially for such cases where parametric analysis is performed, it is preferable to use more simplified model that requires much less computer resource and yet captures the essential features of the nonlinear behavior of URM structures. A composite spring model developed in the precedent work [10] is utilized in this study. A brief explanation on the model follows.

Lateral in-plane stiffness of a solid URM wall, i.e., an URM wall without a perforation, is determined as

$$k = \begin{cases} \dfrac{1}{\dfrac{h^3}{3E_m I_g} + \dfrac{h}{A_v G_m}} & \rightarrow \text{for a cantilevered shear wall} \\ \dfrac{1}{\dfrac{h^3}{12E_m I_g} + \dfrac{h}{A_v G_m}} & \rightarrow \text{for a fixed-fixed shear wall} \end{cases} \quad (1)$$

Where, Em is the modulus of elasticity of masonry, h is the height of the wall, Ig is the moment of inertia, Av is the shear area, and Gm is the masonry shear modulus. This formula is based on the classic theory of bending and shear. The strength of the wall is determined differently for each failure mode. That is, the failure mode of a solid URM wall is determined depending on the vertical compressive force, material strengths, and the shape of the wall [11]. The typical failure modes are rocking,bed-joint sliding, diagonal cracking, and toe crushing. The strength and the hysteresis characteristics of the wall are determined based on the failure mode. Most of the time the failure mode of a solid URM pier is determined as rocking or sliding [2,10]. The formula for calculating the rocking strength of a wall with its length Lw and the height heff is provided from FEMA [11] as

$$Q = 0.9\alpha P_{CE}\left(\frac{L_w}{h_{eff}}\right) \quad (2)$$

Where, PCE is the vertical compressive force and α is a factor regarding the end condition evaluated as 0.5 for fixed-free cantilever wall, or 1.0 for fixed-fixed wall. The bed-joint sliding strength can be calculated as

$$Q = \frac{0.75A_n\left(0.75v_{te} + \frac{P_{CE}}{A_n}\right)}{1.5} \quad (3)$$

Where An is the area of net mortar section, and vte is the average bed-joint shear strength. This formula-base stiffness and strength calculation, however, cannot be applied to a perforated in-plane URM wall. Fig. 3 schematically shows how the composite spring model deals with a perforated wall. In the composite spring model a perforated URM wall is divided into a number of solid wall components. Each wall component is then modeled as a nonlinear spring and connected one another in a series-parallel fashion. The nonlinear springs should be able to describe the lateral strength and the hysteretic behavior of the corresponding component. The end-restraints at the top and bottom of the URM piers (elements 2 to 4 in Fig. 3) should not be assumed either completely fixed or free in this case but should be considered as they have some rotational stiffness as depicted in Fig. 4(a). The value of the rotational stiffness would then depend on the formation of the end conditions. An effective height approach is introduced to account for the rotational stiffness which is less than the ideal fixity. This approach is essentially to make the end boundary conditions remain fixed but instead increase the pier height. That is, the height of an URM pier, h in Eq. (1), is multiplied by r, the effective height factor. The effective height of an URM pier is determined from the end conditions, which are described by the control variables as shown in Fig. 5(b). A regression analysis is performed in such a way that the reference stiffness of a masonry pier is obtained first by performing a plane stress analysis using ABAQUS finite element program [12] and the effective height factor r is obtained by comparing the reference stiffness with Eq.(1), where r*h is used instead of h. The regression analysis performed for identification of the relationship between the control variables and the effective height factor, r, yields the following equation.

$$r = \left[1.005 + 0.19\left(\frac{H_b}{W_p}\right)^{\frac{1}{5}}\right] \times \left[1 + 0.1\alpha^{\frac{1}{4}}\right] \times \left[0.803 + 0.281\left(\frac{W_p}{h_p}\right)\right] \quad (4)$$

The effective height approach described above is based on a simple shear model that assumes the horizontal displacements of each component are due to the corresponding shear force. However, a bending effect also exists in the behavior of an in-plane wall under lateral load applied at the top. This bending effect becomes even larger as the aspect ratio of the wall increases. An additional spring is added to each story of the URM composite spring model accounting for the bending effect, which is represented with elements 6 and 12 in Fig. 3.

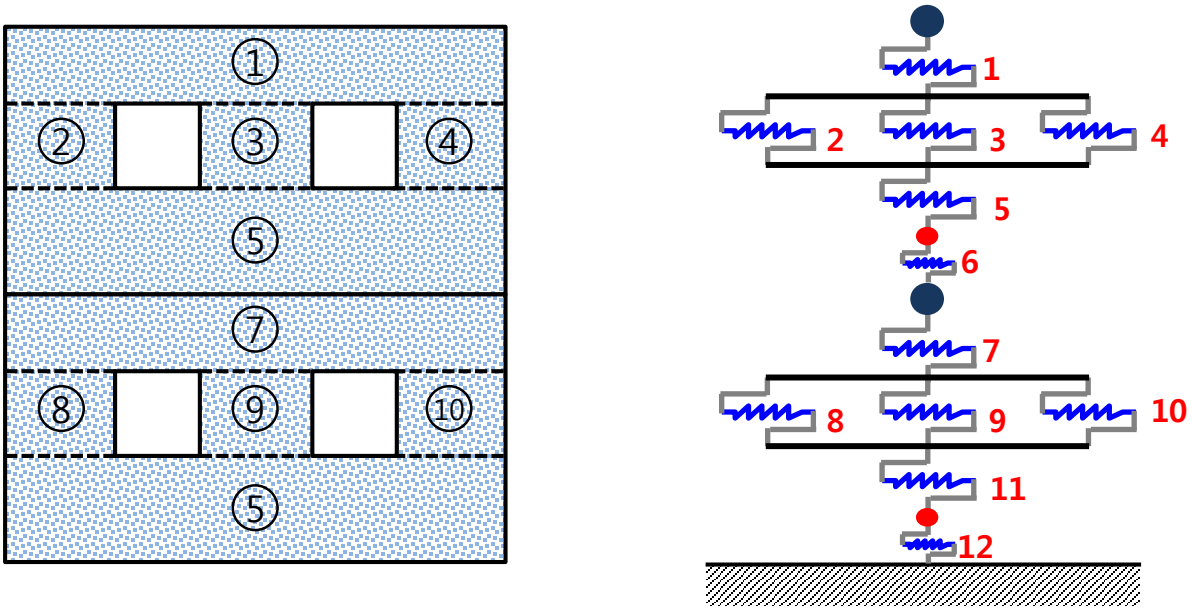

Fig. 3 – Construction of 2D spring model

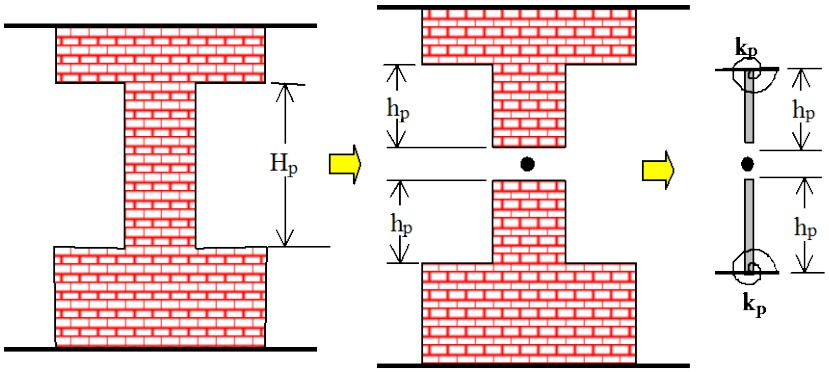

(a) decomposition of pier

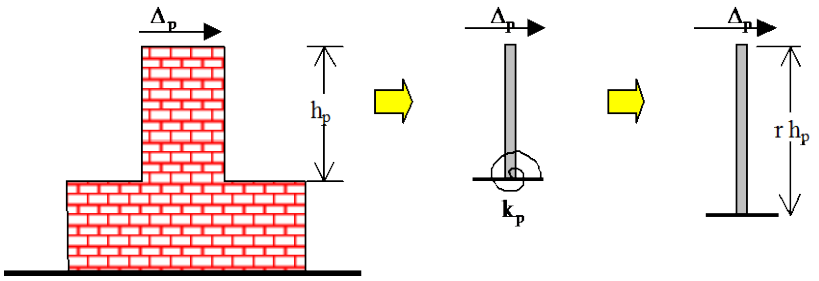

(b) effective height formulation

Fig. 4 – Schematic view of effective length method [10]

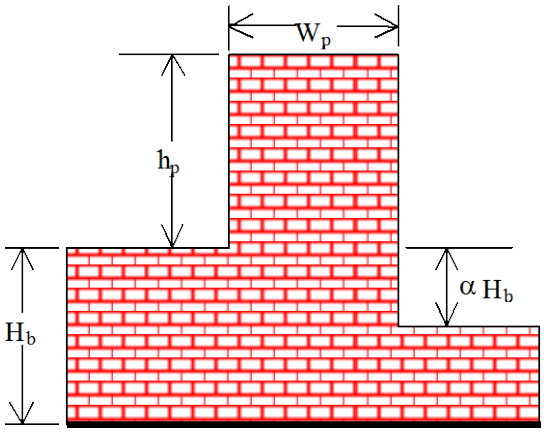

Fig. 5 – Definition of control variables

The modeling of the URM building system using the composite spring model is made in such a way that the in-plane walls and the out-of-plane walls are connected to the diaphragms. It is conservatively considered that the out-of-plane walls are not connected to the in-plane walls. The classic bending theory is applied for calculation of the stiffness of the out-of-plane walls, which are only connected to the diaphragms. The diaphragms, that play roles for a floor and a roof, are modeled to have their axial and shear stiffness. The lateral stiffness of the diaphragms is relatively weak because they are originally designed to withstand only the gravitational loads. In particular, most floors in the old URM buildings distributed in the CSUS region are made of wood. They are simply connected to the walls so the bending cannot be transmitted. Experimental study of a typical wooden floor [13] confirms that the shear stiffness of a diaphragm is much less than the extensional stiffness. The structural properties of the diaphragms are determined following the precedent studies [2,13]. More detailed discussion on the effective height approach and the composite spring model can be found in the reference [10].

4. Seismic damage assessment of URM buildings with different geometric shapes

The effect of the shape variation of URM structures can be investigated by monitoring the seismic response by changing the shape configuration. Variables are selected for description of the URM building shape considering the inventory analysis discussed in Section 2. Fig. 6 shows the definition of the control variables for description of the URM building shape. L and W are the length of the in-plane wall and the out-of-plane wall of the URM building, respectively, and H indicates the story height. Variables a, b, c, d and e define the size and position of the windows. The number of windows in a story is denoted as n, and the perforation ratio is ρ. A number of combinations of the variables are determined with an objective to monitor the trend of the seismic behavior of an URM building upon the variation of the shape as shown in Table 1. C1 to C4 are determined for investigation of the effect of L. Likewise, C5 to C7 are for aspect ratio, C8 to C10 for perforation ratio, and C11 to C13 for number of story. Note that the configuration of each story for multi-story buildings is the same. The baseline case for each group is C2, C6, C9, and C12, which means they have identical configurations. It should be noted that C13 is for a three-story URM building. Although mid-rise URM building includes only one and two story buildings, three-story building is added to the group in order to clarify the effect of the number of stories. The fundamental period, T, of each case is also listed.

Seismic damage analyses are then performed for the 13 combinations (10 combinations considering the baseline combinations are the same). 10 artificial ground motions developed for Memphis [14] which is located in the CSUS region are used as the input earthquake loading (see Fig. 7 for response spectrum of the input ground motions). The input ground motions are scaled such that their spectral acceleration ranges from 0.1g to 3.0g with an increment of 0.1g. A nonlinear time-history analysis is performed using the composite spring model for each of the 10 ground motions that are scaled to a specified spectral acceleration level. DRAIN-2DX [15] is utilized for nonlinear time history analyses where the seismic damage of the structures is obtained. The maximum inter-story drift ratio is monitored for each analysis as the seismic damage measure [2,16].

Fig. 8 shows the damage distribution obtained from the seismic damage analysis for three selected cases – C2, C4 and C11. The dotted lines in the plot indicate four levels of damage state defined in HAZUS, which are slight damage, moderate damage, extensive damage and complete damage. Taking C2 as the baseline case, C4 undergoes noticeably higher seismic damage, showing most of the damages for more than 1.2g spectral acceleration fall in the complete damage range. The variation of the damage distribution also appears larger. The larger lengths of the walls would result in decrease in the stiffness of the out-of-plane walls (OPW) and the diaphragms, which in turn results in larger maximum drift ratio. For the case of a single story building, C11, the seismic damage is significantly less than C2 or C4, showing most of the damages for less than 1.5g spectral acceleration are distributed below the complete damage level. It is obvious from the analysis result presented above that the seismic damage and risk of URM structures with the same classification may not be accurately estimated using a representative single set of fragility curves. For the case where a single or selected multiple URM buildings are examined for the seismic risk, in particular, this approach is even more inappropriate. The physical variation in the URM structures therefore must be explicitly considered for seismic damage assessment and risk analysis.

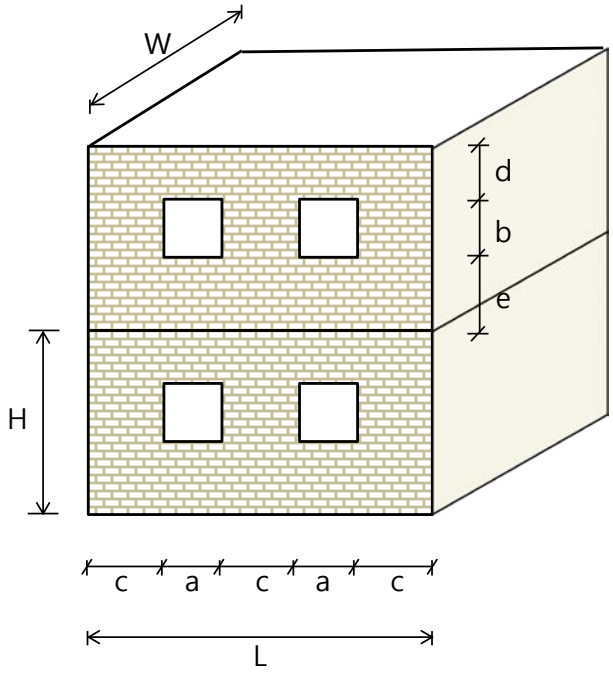

Fig. 6 – Baseline configuration of URM in-plane wall

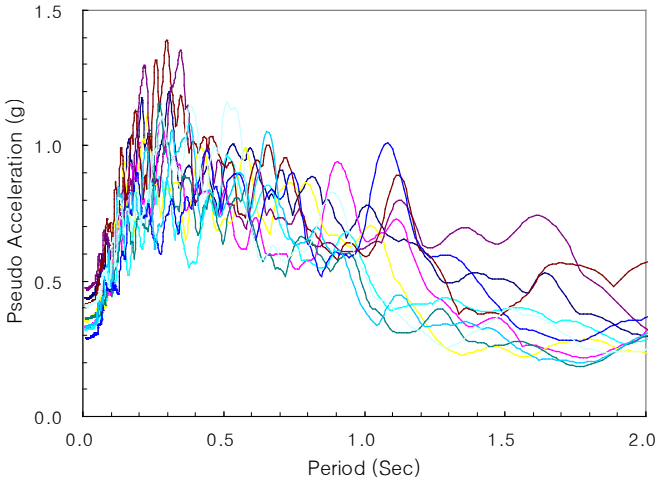

Fig. 7 – Response spectrum of input ground accelerations

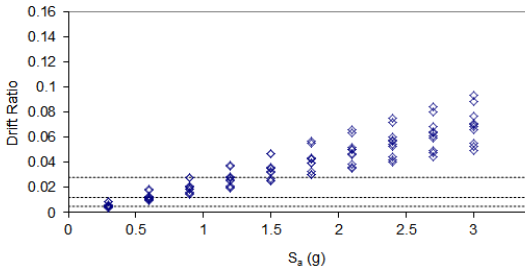

(a) C2

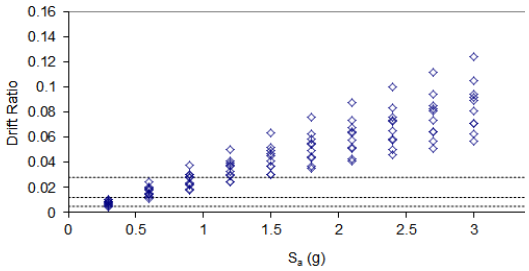

(b) C4

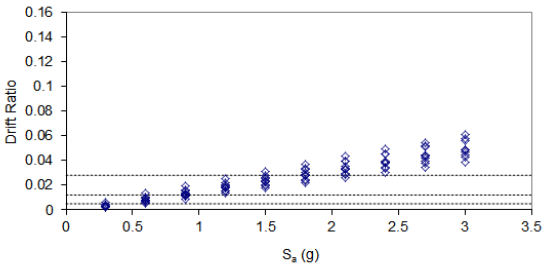

(c) C11

Fig. 8 – Damage trends for selected cases

Table 1 – Configuration of analysis cases

	Length (L, m)				Aspect Ratio (L/W)			Opening Ratio $\left(\rho = \frac{n \times a \times b}{L \times H}\right)$			Number of Story		
	L=7m	L=15m	L=25m	L=35m	L/W=0.5	L/W=1.0	L/W=1.5	ρ=0.05	ρ =0.1	ρ =0.15	1story	2story	3story
	C1	C2	C3	C4	C5	C6	C7	C8	C9	C10	C11	C12	C13
L (m)	7	15	25	35	15	15	15	15	15	15	15	15	15
W (m)	7	15	25	35	7.5	15	22.5	15	15	15	15	15	15
H (m)	3.7	3.7	3.7	3.7	3.7	3.7	3.7	3.7	3.7	3.7	3.7	3.7	3.7
s	2	2	2	2	2	2	2	2	2	2	1	2	3
n	2	4	7	10	4	4	4	2	4	6	4	4	4
Σa	2.16	4.63	7.71	10.79	4.63	4.63	4.63	2.31	4.63	6.94	4.63	4.63	4.63
a (m)	1.08	1.16	1.10	1.08	1.16	1.16	1.16	1.16	1.16	1.16	1.16	1.16	1.16
b (m)	1.2	1.2	1.2	1.2	1.2	1.2	1.2	1.2	1.2	1.2	1.2	1.2	1.2
c (m)	1.61	2.08	2.16	2.20	2.08	2.08	2.08	4.23	2.08	1.15	2.08	2.08	2.08
d (m)	1	1	1	1	1	1	1	1	1	1	1	1	1
e (m)	1.7	1.7	1.7	1.7	1.7	1.7	1.7	1.7	1.7	1.7	1.7	1.7	1.7
ρ	10%	10%	10%	10%	10%	10%	10%	5%	10%	15%	10%	10%	10%
T (s)	0.265	0.287	0.307	0.335	0.33	0.287	0.272	0.289	0.287	0.282	0.166	0.287	0.4

5. Conclusions

This study analytically investigates the effect of geometric variation of URM buildings on their seismic behavior. Variables describing the geometric variation are defined by utilizing the URM inventory data for the CSUS region. A composite spring model is utilized for effective computer analyses of URM buildings. A series of sensitivity analyses are performed by developing the seismic distribution curves for URM buildings with different physical configurations and the following conclusions are made.

Other conditions being the same, increase in the length of an URM building leads to increase in the seismic vulnerability. This is because the seismic failure of URM buildings is defined by the excessive lateral

displacement of the diaphragms and OPWs. It should be noted that the torsional behavior of URM buildings due to the uncertain earthquake direction could presumably affect the seismic performance. It is suggested that the future study on the seismic risk assessment of URM structures should consider the torsional effect.

It was expected that the perforation ratio of the IPWs would affect the seismic performance level of URM buildings but the analysis results shows that it does not have much effect on the seismic vulnerability. The stiffness degradation of the IPWs due to the perforation effect does not significantly contribute to the overall seismic performance because the diaphragms and the OPWs responses have much higher order than the IPWs responses. More refined identification of the OPW behavior and the connections behavior between IPWs and OPWs is needed for more accurate seismic performance evaluation of URM structures.

It is observed that the two-story building undergoes higher seismic damage than the single-story building. This is due to the flexural effect and the story response amplification of the buildings with higher stories. It should be noted that the difference in the seismic vulnerability between the single-story building and the two-story building is even larger than the difference between the two-story building and the three-story building. This implies that sharing a set of fragility curves for single-story buildings and two-story buildings may not be adequate but should be considered separately for representation of the seismic risk.

Considering the analysis results in this study, using the representative fragility curves for low-rise URM buildings is not adequate because significant variation exists in the seismic performance level of the buildings in the category. The geometric variation of the URM buildings must be considered for the seismic risk assessment of low-rise URM buildings, especially when the target system is an individual or comprised of a selected group of buildings.

6. Acknowledgements

This work was supported by the National Research Foundation of Korea (NRF) grant funded by the Korea government (MSIP) (No. 2014R1A2A2A01007654).

7. References

[1] S. French S, Olshansky R (2000): Inventory of Essential Facilities in Mid-America, *Mid-America Earthquake Center Project SE-1 Final Report.*

[2] Park J, Towashiraporn P, Craig JI, Goodno BJ (2009): Seismic fragility analysis of low-rise unreinforced masonry structures, *Engineering Structures*, **31**(1), 125-137.

[3] NIBS - National Institute of Building Science (2003): HAZUS-MH MR3 Multi-Hazard Loss Estimation Methodology: Earthquake Model, *Technical Manual*, Washington DC.

[4] Park J, Towashiraporn P (2014): Rapid seismic damage assessment of railway bridges using the response-surface statistical model, *Structural Safety*, **47**(2), 1-12.

[5] Seo J, Linzell DG (2013): Use of response surface metamodels to generate systems level fragilities for existing curved steel bridges, *Engineering Structures*, **52**, 642-653.

[6] Bothara JK, Dhakal RP, Mander JB (2010): Seismic performance of an unreinforced masonry building: an experimental investigation, *Earthquake Engineering and Structural Dynamics*, **39**(1), 45-68.

[7] Agnihotri P, Singhal V, Rai DC (2013): Effect of in-plane damage on out-of-plane strength of unreinforced masonry walls, *Engineering Structures*, **57**, 1-11.

[8] Bruneau M (1994): Seismic Evaluation of Unreinforced Masonry Buildings – a State-of-the-Art Report, *Canadian Journal of Civil Engineering*, **21**(3), 512-539.

[9] Shing PB, Klingner RE (1998), Nonlinear Analysis of Masonry Structures, *Structural Engineering World Wide T125-2*, Elsevier Science Ltd.

[10] Craig JI, Goodno BJ, Towashiraporn P, Park J (2002): Response modification applications for essential facilities, *Mid-America Earthquake Center Project ST-4 Final Report.*

[11] ASCE (2000): FEMA 356. Prestandard and commentary for the seismic rehabilitation of buildings, Publication No. 356, *Federal Emergency Management Agency*, Washington DC.

[12] ABAQUS (2011): ABAQUS documentation, *Dassault Systemes*, Provindence, RI, USA.

[13] Yi T (2004): Experimental investigation and numerical simulation of an Unreinforced masonry structure with flexible diaphragms, *Ph.D. Thesis*, Georgia Institute of Technology.

[14] Wen YK, Wu CL (2001), Uniform hazard ground motions for Mid-America cities, *Earthquake Spectra*, **17**(2), 359-384.

[15] Prakash V, Powell GH, Campbell S (1993): DRAIN-2DX base program description and user guide, Ver. 1.10, Department of Civil Engineering, University of California, Berkeley, CA.

[16] Ellingwood BR (2001): Earthquake risk assessment of building structures, *Reliability Engineering and System safety*, **74**(3), 251-262.